

Cover Page for

## **FINAL REPORT**

**Pulsed Artificially Created Electrojet**  
Contract No. HR0011-09-C-0103

February 2010

Submitted by:

Chia-Lie Chang, BAE Systems Program Manager

Distribution List:

- (a) Douglas Kirkpatrick, DARPA/STO
- (b) Patricia Matyskiela, DARPA/CMO
- (c) Patrick Bailey, ADPM, DARPA/STO
- (d) Craig Selcher, COR, ONR/NRL
- (e) Robert Cowan, SPC/DARPA/STO-SETA
- (f) Carlton Gibbs, SPC/DARPA/STO-SETA
- (g) Jessica Blum, BAE Systems Contracting Officer
- (h) Michael Frankhuizen, BAE Systems Contracting Officer

Sponsored by:

Defense Advanced Research Projects Agency  
Strategic Technology Office (STO)  
Program: Pulsed Artificially Created Electrojet  
ARPA Order No. X126/00, Program Code: 7F40  
Issued by DARPA/CMO under Contract No. HR0011-09-C-0103

The views and conclusions contained in this document are those of the authors and should not be interpreted as representing the official policies, either expressly or implied, of the Defense Advanced Research Projects Agency or the U.S. Government.

# Report Documentation Page

*Form Approved*  
*OMB No. 0704-0188*

Public reporting burden for the collection of information is estimated to average 1 hour per response, including the time for reviewing instructions, searching existing data sources, gathering and maintaining the data needed, and completing and reviewing the collection of information. Send comments regarding this burden estimate or any other aspect of this collection of information, including suggestions for reducing this burden, to Washington Headquarters Services, Directorate for Information Operations and Reports, 1215 Jefferson Davis Highway, Suite 1204, Arlington VA 22202-4302. Respondents should be aware that notwithstanding any other provision of law, no person shall be subject to a penalty for failing to comply with a collection of information if it does not display a currently valid OMB control number.

1. REPORT DATE <b>FEB 2010</b>	2. REPORT TYPE	3. DATES COVERED <b>00-00-2010 to 00-00-2010</b>			
4. TITLE AND SUBTITLE <b>Pulsed Artificially Created Electrojet</b>		5a. CONTRACT NUMBER			
		5b. GRANT NUMBER			
		5c. PROGRAM ELEMENT NUMBER			
6. AUTHOR(S)		5d. PROJECT NUMBER			
		5e. TASK NUMBER			
		5f. WORK UNIT NUMBER			
7. PERFORMING ORGANIZATION NAME(S) AND ADDRESS(ES) <b>BAE Systems, United Kingdom, ,</b>		8. PERFORMING ORGANIZATION REPORT NUMBER			
9. SPONSORING/MONITORING AGENCY NAME(S) AND ADDRESS(ES)		10. SPONSOR/MONITOR'S ACRONYM(S)			
		11. SPONSOR/MONITOR'S REPORT NUMBER(S)			
12. DISTRIBUTION/AVAILABILITY STATEMENT <b>Approved for public release; distribution unlimited</b>					
13. SUPPLEMENTARY NOTES					
14. ABSTRACT					
15. SUBJECT TERMS					
16. SECURITY CLASSIFICATION OF:			17. LIMITATION OF ABSTRACT <b>Same as Report (SAR)</b>	18. NUMBER OF PAGES <b>16</b>	19a. NAME OF RESPONSIBLE PERSON
a. REPORT <b>unclassified</b>	b. ABSTRACT <b>unclassified</b>	c. THIS PAGE <b>unclassified</b>			

## Motivation

The objective of the PACE project is to determine the HED moment required to achieve nT magnetic field at distances from .5-1 Mm from the location of the ground based HED at locations near the magnetic equator. Significant advantage can be gained if the HED radiates in a sneak-through or partial sneak-through mode, in which the observed signal from a magnetic dipole ground return antenna creates a magnetic field that scales as  $1/R^2$  (naked current) or  $1/R^\alpha$  where  $\alpha < 3$  instead of the usual  $1/R^3$  for dipole fields. Since standard magnetic dipole loop antennae (vertical dipole, horizontal current) induce an opposite dipole in the ground, resulting in fields that drop off as  $1/R^4$ , the PACE antenna has a strong scaling advantage over them.

## Results Summary

Using a 220m ground return antenna carrying 8 A of current ( $IL=1760$  Am) at 217 Hz, we generated signal of 38.6 pT at 884 m altitude, scaling as  $1/R^{2.4}$ . This implies that the required nT fields at 0.5-1 Mm can be achieved near the magnetic equator with antenna  $IL$  of a few A-Mm.

## Implications to the Artificially Created Electrojet Concepts (ACE or PACE)

These concepts rely on the fact that in the magnetic equator region the direct far magnetic field generated by a ground based HED, CW or pulsed, is smaller than the far field due to the induced current in D/E ionospheric region above the HED. This effect is due to the fact that as seen in Figure 1 the ionospheric conductance varies strongly with geomagnetic latitude.

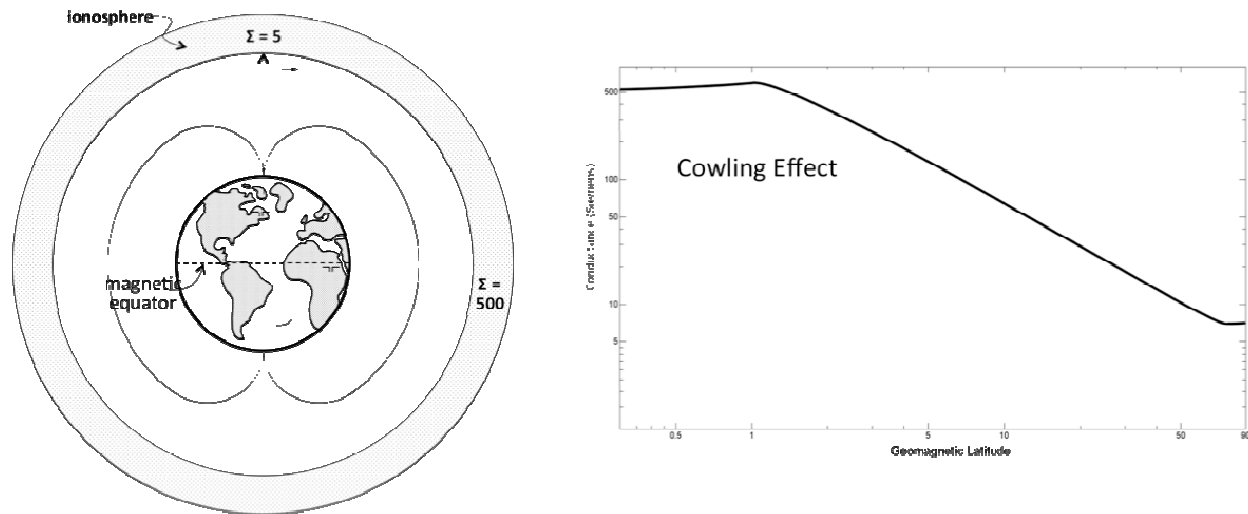


**Fig-1. Distribution of the D/E Region Conductance vs. Magnetic Latitude**

Referring to Figure 2 and for frequencies below the Earth-Ionosphere waveguide cutoff ( $\sim 8$  Hz) the magnetic field  $B(R)$  at a distance  $R$  from the HED due to the induced ionospheric current  $I$  at altitude  $z$  and over a size  $L$  comparable to  $z$  (dipole field) is given by

$$B(R) \approx \mu_o \frac{IL}{2\pi R^2} \quad (1)$$

The value of the current  $I$  driven by a magnetic field  $B_T$  due to the HED transmitter at a height  $z$  is given by

$$I \approx cB_T \Sigma L \quad (2)$$

In Eq. (2)  $\Sigma$  is the ionospheric conductance. From Eqs (1) and (2) we find that

$$B(R)/B_T \approx \frac{Z_0 \Sigma}{2\pi} (L/R)^2 \approx 3 \times 10^4 (L/R)^2 \quad (3)$$

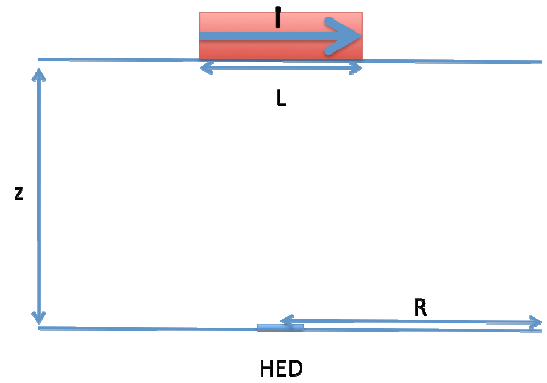


Figure 2: ACE – PACE Concept

In Eq. (3)  $Z_0 = 377$  ohm and  $\Sigma = 500$  Siemens.

The experimental results help us explore the requirements for achieving nT fields at .5 to 1 Mm distances. Following the experiment results we can write the value of  $B_T$  as

$$B_T(z) = B_{\text{exp}}(z = 1\text{km})(1\text{km}/z)^\alpha \quad (4)$$

In Eq. (4)  $B_{\text{exp}} \approx .04$  nT as measured at 1 km height,  $z \approx 90$  km the ionospheric height and  $\alpha$  is the scaling factor that varies between 2 and 3 and was found to be approximately 2.4 in the experiment. Assuming a ground HED moment  $p$  and normalizing it to the value of 2 A-km used in the experiment we find that

$$B(R) \approx 1.2(Mm/R)^2 (p/1A - Mm)(km/z)^{\alpha-2} nT \quad (5)$$

In deriving Eq. (5) we assumed that  $L \approx z$ .

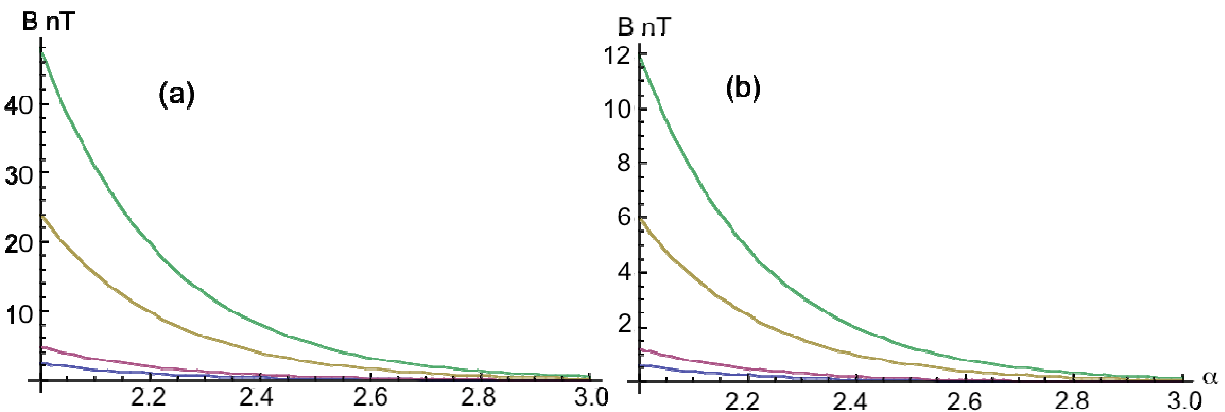


Fig-3. The magnetic field at 0.5 Mm (a) and 1.0 Mm (b) as a function of the scaling factor  $\alpha$ , for four values of  $IL$ : 1, 2, 5, and 10 A-Mm.

Figure 3 shows the important conclusions of the experiment for generating nT fields at Mm distances. Figure 3a and 3b show the magnetic field at a distance of .5 and 1 Mm respectively,

for values of ground HED 1, 2, 5 and 10 A-Mm as a function of the value of  $\alpha$ . Notice that for a value of  $\alpha \approx 2.4$ , nT fields can be achieved with values of  $p$  of the order of few A-Mm.

### Antenna Configuration

A low frequency vertical magnetic dipole antenna (horizontal wire) will induce on the ground a dipole opposite to that created by the antenna. The image dipole penetrates into the ground to a distance  $d \approx L\delta/(L + \delta)$ , where  $L$  is the linear length of the antenna and  $\delta = c/\sqrt{2\pi\sigma\mu\omega}$  is the skin depth (cf. Fig-4). At distances  $R \gg d$  the two opposing dipoles cancel to third order, and result in fields that fall off as  $1/R^4$  (cf. Greifinger 1979, eq. 17; see also Wait 1951, eq. 32).

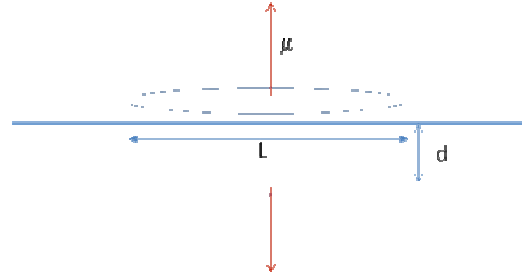
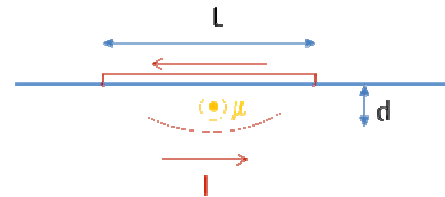


Fig 4. A vertical magnetic dipole antenna (horizontal wire) and its ground image. The depth of the ground image is  $d \approx 2L\delta/(L + \delta)$ , where  $\delta$  is the skin depth.

The PACE antenna is a ground return antenna, meaning that the image current is the same as the return current (cf. Fig-5), so that the near zone fields fall off as  $1/R^3$ . Furthermore, since the return current has to diffuse into the ground, we expect that for driving current with period  $T \gg \tau_D$  (i.e. frequencies  $f \ll 1/\tau_D$ ) the field will scale as  $1/R^2$ , and for frequencies  $f \gg 1/\tau_D$  we expect that the field will scale as  $1/R^3$ . Several antenna configurations are possible, and we have calculated the return current configuration as a function of depth and time for several of them (cf. Appendix A).

Fig 5. The PACE ground return antenna. The induced current is also the return current so only one dipole is produced, albeit a horizontal one.



### Experimental Results

We tested the PACE antenna concept using a 220m antenna over ground with conductivity  $\sigma=0.02$  Siemens/m, which gives us a diffusion time of  $\tau = L^2/D = L^2\mu\sigma = 1.2ms$ . We drove 8A of current at frequencies from 217 Hz to 10 kHz, both in pulsed and sine mode, and measured the magnetic field at three altitudes, at 91m, 274m, 579m, and 884m (cf. Appendix B for details of the operation).

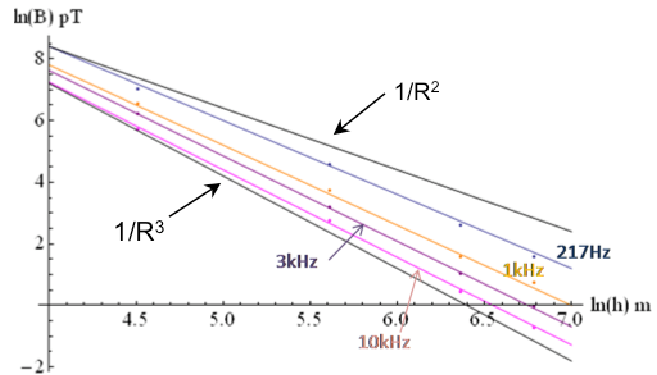


Fig 6. The value of the measured magnetic field strength, in pT, versus height, for 217Hz, 1kHz, 3kHz and 20kHz from top to bottom respectively. The slopes of the graphs are -2.40, -2.60, -2.77, and -2.84 respectively. The black lines at the very top and bottom have slopes -3.0 and -2.0 respectively, for reference.

Figure 6 shows the measured magnetic field as a function of altitude for each of the four frequencies. The values are given in Table 1. The slope of each plot gives the scaling exponent. The two black lines at the top and bottom are the  $-3.0$  ( $1/R^3$ ) and  $-2.0$  ( $1/R^2$ ) lines respectively,

for reference. We see that for high frequencies, the measured magnetic field scales approximately as  $1/R^3$ , but as the frequency is decreased, the scaling approaches  $1/R^2$ .

Figure 7 shows the scaling exponent as a function of the timescale ratio  $\tau_D / T = f * \tau_D$ . The measured data is fitted with a hyperbolic tangent function (since the curve is expected to asymptote at 3.0 and 2.0 for a dipole and naked current respectively). Extrapolating to a nominal 10Hz frequency we see that the magnetic field for this diffusion time would scale as  $1/R^{2.2}$ .

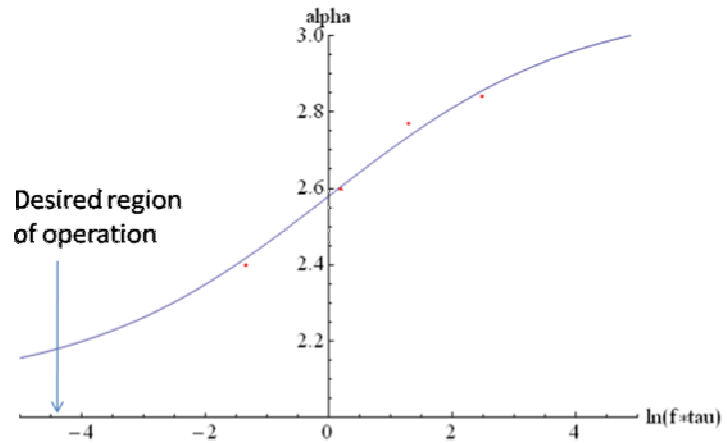


Fig 7. **The scaling of the exponent,  $\alpha$ , as a function of  $f\tau_D$ , where  $\tau_D$  is the diffusion time, given by  $\tau_D = L^2 / D = L^2 \mu \sigma$ . The curve is a hyperbolic tangent fit. For the current antenna with  $\tau_D = 1.2\text{ms}$  the fit gives an exponent of  $\alpha = 2.2$  for  $f = 10\text{Hz}$ .**

Using the measured scaling of  $1/R^{2.4}$ , we calculate that the required nT field can be generated at 0.5-1 Mm distance with an antenna IL of a few A-Mm (cf. Fig. 3).

**Table-1**

Field Strength at 217 Hz - calculated using quickplot.m demodulation function w/integration time of 10 sec

Antenna Current =		8.9	A rms		217 Hz			exponent	-2.404
Altitude	Hns (pT)	Hew(pT)	Hhor (pT)	Ft (pT/A)	ln(altitude)	ln(Ft)	const	1.79E+01	
91	9457	3066	9941.59	1117.033	4.51086	7.018431	7.10E+00		
274	726	503	883.2242	99.23867	5.613128	4.597528	4.45E+00		
579	118.6	26.8	121.5903	13.66183	6.361302	2.614606	2.65E+00		
884	38.3	19.5	42.97837	4.82903	6.784457	1.574646	1.63E+00		

Field Strength at 1 kHz - calculated using quickplot.m demodulation function w/integration time of 10 sec

Antenna Current =		6.26	A rms		1 kHz			exponent	-2.604
Altitude	Hns (pT)	Hew(pT)	Hhor (pT)	Ft (pT/A)	ln(altitude)	ln(Ft)	const	18.3	
91	3300	2900	4393.177	701.7854	4.51086	6.553628	6.553722		
274	221	148	265.9793	42.48871	5.613128	3.749238	3.683414		
579	26	15	30.01666	4.794994	6.361302	1.567572	1.735168		
884	13	2	13.15295	2.10111	6.784457	0.742466	0.633274		

Field Strength at 3 kHz - calculated using quickplot.m demodulation function w/integration time of 10 sec

Antenna Current =		4.12	A rms		3 kHz			exponent	2.774
Altitude	Hns (pT)	Hew(pT)	Hhor (pT)	Ft	ln(altitude)	ln(Ft)	const	18.74	
91	2054	410	2094.52	508.3788	4.51086	6.231227	6.226876		
274	95.7	26	99.169	24.07014	5.613128	3.180972	3.169183		
579	10.8	3.7	11.41622	2.770926	6.361302	1.019182	1.093747		
884	3.99	0.33	4.003623	0.971753	6.784457	-0.02865	-0.08008		

Field Strength at 10 kHz - calculated using quickplot.m demodulation function w/integration time of 10 sec

Antenna Current =		1.56	A rms		10 kHz			exponent	2.843
Altitude	Hns (pT)	Hew(pT)	Hhor (pT)	Ft	ln(altitude)	ln(Ft)	const	18.58	
91	326	341	471.7595	302.4099	4.51086	5.711783	5.755626		
274	21.6	10.7	24.10498	15.45191	5.613128	2.737733	2.621877		
579	2.16	1.17	2.456522	1.574694	6.361302	0.454061	0.494817		
884	0.63	0.25	0.677791	0.487024	6.784457	-0.71944	-0.70821		
884	0.83	0.14	0.841724						

**References**

Greifinger, Carl, Feasibility of Ground-Based Generation of Artificial Micropulsations, *J. Geophys. Res.* 77, 6761 (1972).

Wait, James R., The Magnetic Dipole Over the Horizontally Stratified Earth, *Can. J. Phys.* 29, 577 (1951).

## Appendix A

# Ground Return Antenna Configurations

The objective of the project is to calculate the fields produced by an antenna of length  $L$  whose return current flows through a homogeneous half space of conductivity  $\sigma$ . Calculating the fields is equivalent to calculating the currents, so we limit ourselves to calculating the return current of such an antenna.

Given a driving current on the surface of a conductor of conductivity  $\sigma$  and magnetic permeability  $\mu$ , the magnetic field produced by the driving current will diffuse into the conductor according to

$$\frac{1}{\mu\sigma} \nabla^2 \vec{H} = \frac{\partial \vec{H}}{\partial t}$$

which we solve in a number of geometries, depending on the requirements of the problem. The current density is then given by

$$\vec{j} = \vec{\nabla} \times \vec{H}$$

### 1D Solution with Finite Depth

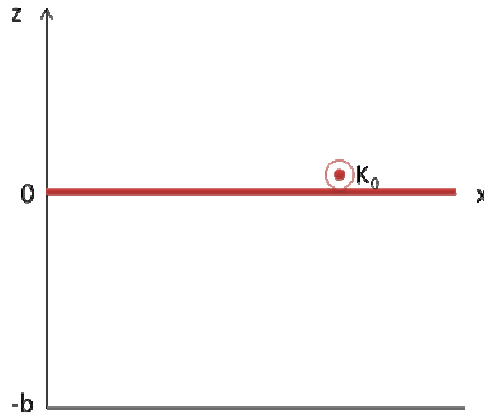


Figure 1. The 1D configuration of an infinite current sheet  $K_0$  on the surface of a homogeneous conductor of depth  $b$ .

The 1D solution corresponding to an infinite sheet of current density  $-K_0 \hat{y}$  over ground of depth  $b$  (cf. Figure 1) has been calculated by Papadopoulos<sup>[1]</sup>, and is given by:

$$\frac{H_x(z,t)}{K_0} = 1 + \frac{z}{b} + 2 \sum_{n=0}^{\infty} \frac{1}{n\pi} \sin\left(\frac{n\pi z}{b}\right) e^{-t/\tau_n}$$

$$\frac{J_y b}{K_0} = 1 + 2 \sum_{n=0}^{\infty} \cos\left(\frac{n\pi z}{b}\right) e^{-t/\tau_n}$$

Where  $\tau_n = \frac{\mu\sigma b^2}{(n\pi)^2}$  is the decay time of mode  $n$ . The current sheet  $-K_0 \hat{y}$  is considered to be turned on suddenly at  $t=0$ . Plots of the field  $H$  and current density  $J$  are given below as a function of  $z$  at

different times  $t$ . At  $t \rightarrow 0$  the return current is concentrated in a shallow range around  $z=0$ . As  $t \rightarrow \infty$  the current density becomes constant across the conductor.

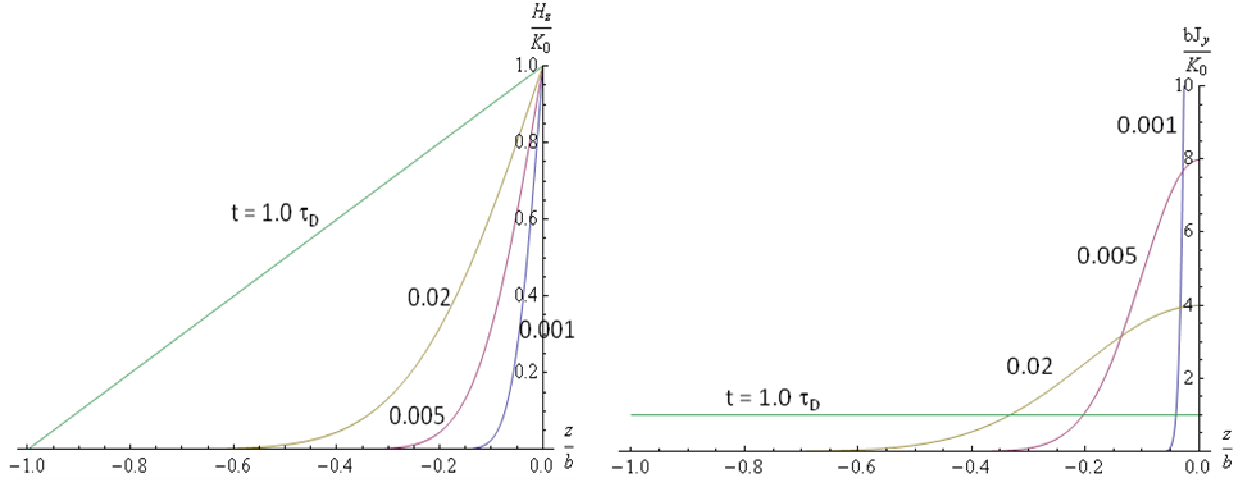


Figure 2. Plots of the field  $H_x$  and current density  $J_y$  as a function of depth for the 1D solution with sudden turn-on.

### 1D solution with infinite depth, slow turn-on

This is the same configuration as Figure 1 above, except that the conductor extends to  $z \rightarrow -\infty$ . In addition, the driving current is given by  $K_0(1 - e^{-t/\tau_R})$  instead of being turned on instantly at  $t=0$ . In that case the field and current are given by

$$H_x(z, t) = \sum_{n=1}^{\infty} \frac{(-1)^{n+1} t^n}{\tau_R^n} \left[ \frac{{}_1F_1(1/2 - n, 3/2, -z^2/4Dt)}{\Gamma(n+1)} - \frac{z}{\sqrt{Dt}} \frac{{}_1F_1(1/2 - n, 3/2, -z^2/4Dt)}{\Gamma(n+1/2)} \right]$$

$$J_y(z, t) = \sum_{n=1}^{\infty} \frac{(-1)^n t^n}{\tau_R^n} \left[ \frac{nz}{Dt} \frac{{}_1F_1(1 - n, 3/2, -z^2/4Dt)}{\Gamma(n+1)} - \frac{1}{\sqrt{Dt}} \frac{{}_1F_1(1/2 - n, 3/2, -z^2/4Dt)}{\Gamma(n+1/2)} - \frac{(n-1/2)z^2}{3(Dt)^{3/2}} \frac{{}_1F_1(3/2 - n, 5/2, -z^2/4Dt)}{\Gamma(n+1/2)} \right]$$

Where  ${}_1F_1$  is the confluent hypergeometric function. Plots of the current density as a function of  $z$  for different times are given in Figure 3. We see that they are similar to the current distributions in the finite depth case, except that they extend to infinity, and it takes an infinite time to become flat.

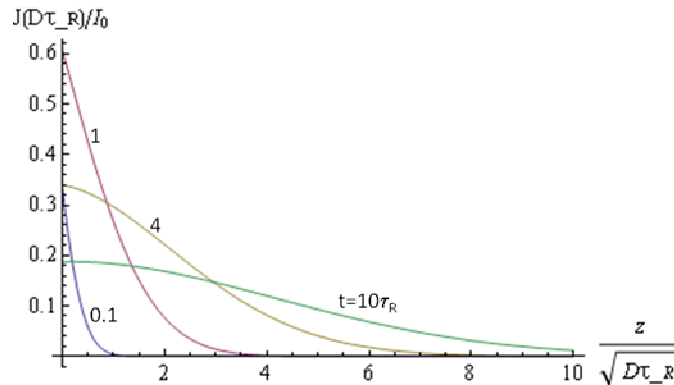


Figure 3. A plot of the current density as a function of depth at different times, for the unlimited depth solution.

As a check, we can see that the integral of the current density over all space gives the driving current at all times:

$$\int_0^{\infty} J_y dz = \sum_{n=1}^{\infty} \left( \frac{-t}{\tau_R} \right)^n \frac{-1}{\Gamma(n)} = 1 - e^{-t/\tau_R}$$

## 2D Solution with sudden turn-on, short antenna

This is a 2D strip of current of length  $2b$  along  $y$ , with infinite width along  $x$  (cf. Figure 4). Current flows in the  $y$  direction (hence “short” antenna; if the current were flowing in the  $x$  direction it would make a “long” antenna). We assume that the driving current is turned on at  $t=0$ .

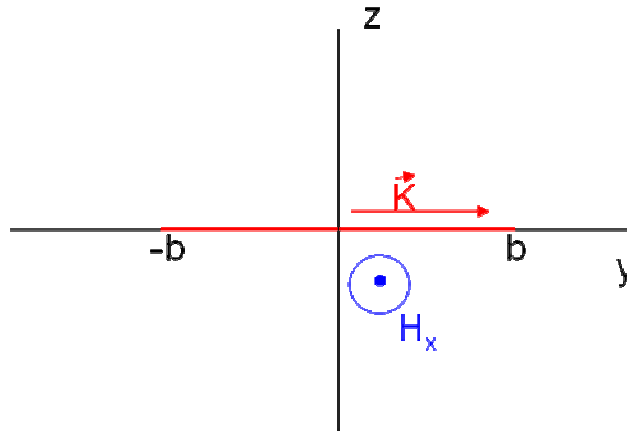


Figure 4. The short 2D antenna configuration. The long 2D antenna would have the current  $K$  flowing in the  $x$  direction.

In this case the field and current are given by

$$\frac{\partial H_x}{\partial t} = \frac{1}{\mu\sigma} \nabla^2 H_x$$

$$\vec{j} = \vec{\nabla} \times \vec{H} = \frac{\partial H_x}{\partial z} \hat{y} - \frac{\partial H_x}{\partial y} \hat{z}$$

So the current has both an  $-x$  and a  $-y$  component. The solutions to the equations are given by

$$H_x(y, z, t) = -\frac{K}{b} \operatorname{Erfc}\left(\frac{-z}{2\sqrt{Dt}}\right) \left[ \operatorname{Erf}\left(\frac{b-y}{2\sqrt{Dt}}\right) + \operatorname{Erf}\left(\frac{b+y}{2\sqrt{Dt}}\right) \right]$$

$$J_y = \partial_z H_x = \frac{2K}{b\sqrt{\pi Dt}} e^{-z^2/4Dt} \left[ \operatorname{Erf}\left(\frac{b-y}{2\sqrt{Dt}}\right) + \operatorname{Erf}\left(\frac{b+y}{2\sqrt{Dt}}\right) \right]$$

$$J_z = -\partial_y H_x = -\frac{K}{b\sqrt{\pi Dt}} \operatorname{Erfc}\left(\frac{-z}{2\sqrt{Dt}}\right) \left( e^{-(b-y)^2/4Dt} - e^{-(b+y)^2/4Dt} \right)$$

where Erf and Erfc are the error function and complementary error function respectively, and  $D=1/\mu\sigma$  is the diffusion coefficient. The natural unit of length for the system is  $b$ , and the natural

unit of time the diffusion time across  $b$ , given by  $\tau_D = \sqrt{b^2 / D} = \sqrt{\mu\sigma b^2}$ . Figure 5 shows the currents  $J_y$  and  $J_z$  as a function of  $y$  and  $z$  at time  $t=0.3\tau_D=0.3\mu\sigma b^2$ .

The above expressions were derived in the early-time approximation, in which  $l_D = \sqrt{Dt} \ll b$ , i.e. early enough so that the currents have diffused only a fraction of the current length  $b$ .

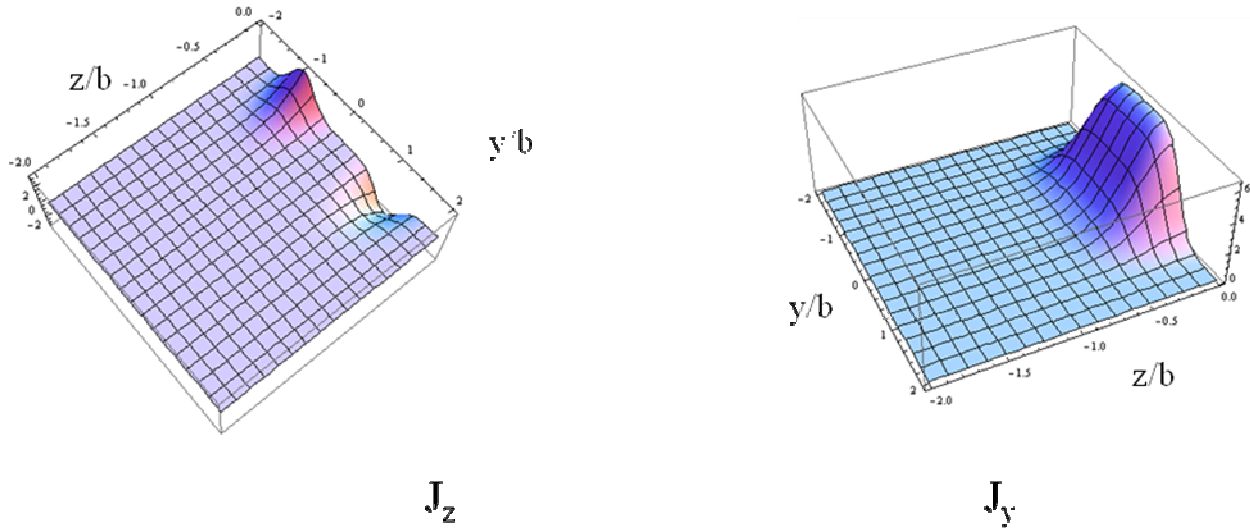


Figure 5. Plots of the return current system produced by the short 2D grounded antenna. We see the current rising at  $-b$ , and sinking at  $b$ , as expected.

## References

- [1] Papadopoulos, Dennis, Computation of seawater response to steady state or pulse current (HED) source, BAE report (2008).

## Appendix B

---

---

### CAMPAIGN TITLE: PACE FLIGHT TEST

---

---

#### Objectives:

- Measure the magnetic field response above a multi-wire grounded dipole antenna driven by pulsed and CW Very Low Frequency (VLF) currents.

#### Overview:

During the PACE flight test, we set up a multi-wire grounded dipole antenna and measured the magnetic fields above the antenna using a three axis sensor package suspended by a tether from a helicopter. Measurements were made as a function of altitude above the antenna for pulsed and CW VLF operation. Simultaneous measurements of the antenna current and voltage were made, as well as reference magnetic field measurements on the ground.

#### Site:

Windy Acres Farm  
3946 Robinson Neck Rd  
Taylors Island MD 21669

#### Campaign Partners:

HeloAir

#### BAE Personnel:

Jim Dolan  
Michael Beversluis  
Hira Shroff

#### Test Equipment:

##### Aircraft:

Bell Long Ranger III

##### Airborne Magnetic field sensor system:

###### On Sensor Platform:

3 BF-6 Sensors.  
3x 10 m, 8 conductor Cable  
EMI battery box  
100 m 14 conductor cable  
Female Tajimi to BNC adaptor

###### In Aircraft:

Dell Latitude D620  
NI PXI-1031B Chassis w/PXI-8310 Interface  
NI PXI-4462 D/A Card  
NI PXI-6653 Timing Card  
Symmetricom bc637PCI GPS Card  
GPS Antenna

100' x 1/2" dia Synthetic Cable Tether w/100 m 14 ckt cable attached

Antenna:

Transmitter:

Yamaha EF3000iSE Generator  
Crown XTi 4000 amplifier  
220 m 16 Ga wire  
4 x 8' ground stakes  
Balanced-XLR converter

Control/Monitoring System

HP33120A Programmable Function Generator  
Dell Optiplex GS280 Computer (PizzaBox)  
M-Audio Delta1010 Digitizer  
Datum ExacTime 2000 GPS Timing Module  
GPS Antenna  
Pearson 5046 Current Monitor

Reference Station:

Dell Latitude D620  
Data Translation DT9816 USB Digitizer  
3 BF-6 Sensors  
3 10 m 8 ckt cables  
EMI Battery Box  
100 m 14 ckt STP Cable

**Day 1:**

**Antenna Installation**

A single strand of 16 ga wire was strung between each of the pairs of 5/8" x 8' stakes previously installed in the northern part of Windy Acres Farm and common supply and return wires were connected from the amplifier at the generator end of the antenna array.



Figure 6

### Ground Test

A three axis sensor system, with the coordinates aligned such that the x axis was parallel to the antenna was set up 100 m from the center of the antenna (see Figure 1). This is the same distance as used during preliminary tests in January. The attached drawings titled 'PACE Ground Test' and 'PACE Reference Station' show how the equipment is connected. The measured magnetic fields at the reference station were compared to the fields measured in January verifying that the antenna was operating correctly. The sequence of signals used to drive the antenna is shown in Table 1:

Duration (sec)	Mode	Frequency	Voltage (Vrms)	Current (Irms)
10	Off	-	-	-
70	Square	217 Hz	69	9.6

10	Off			
70	Square	217 Hz	69	9.6
10	Off			
70	Square	217 Hz	69	9.6
10	Off			
70	Square	217 Hz	69	9.6
10	Off			
50	Sine	1000 Hz	48	6.2
50	Sine	3000 Hz	47	4.1
50	Sine	10000 Hz	47	1.6

Table 1

**Day 2:**

The equipment from the previous test was set up and tested to determine that it was functioning as before. At this point, HeloAir was contacted and asked to bring the helicopter in from Richmond. BAE Systems personnel set up orange safety cones in a 50' square at the landing area, located at approximately 38° 26' 15.89" N, 76° 17' 27.96" W (Figure 2).

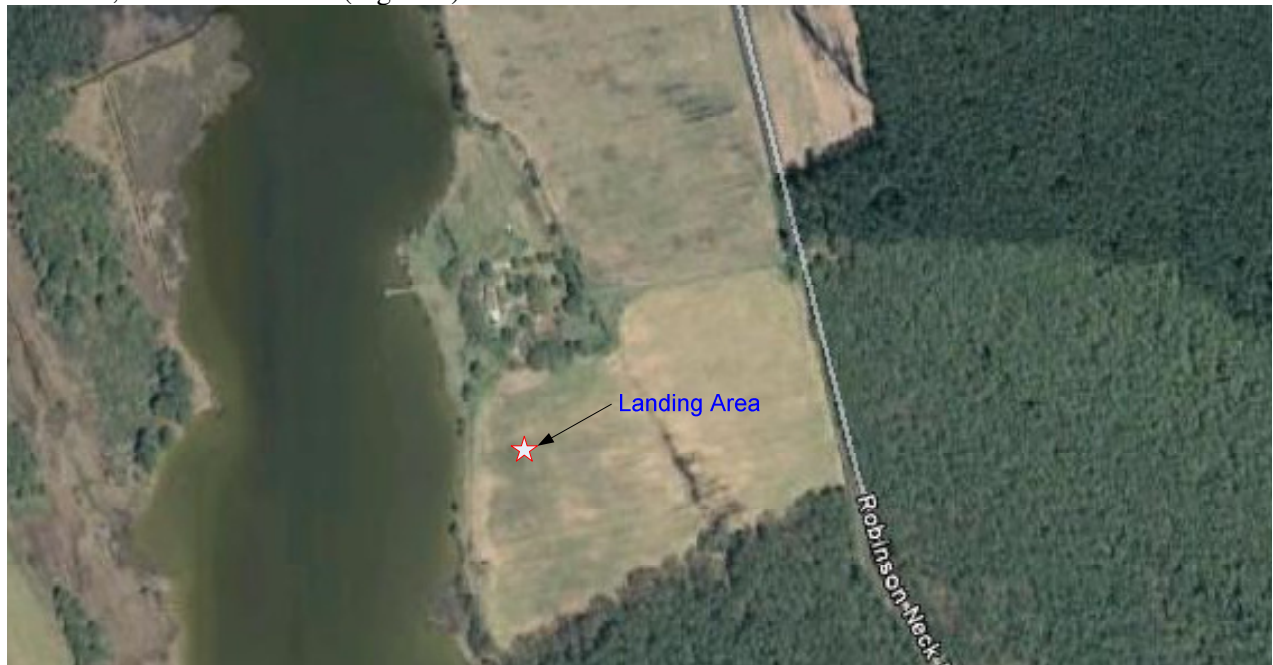


Figure 7

## Flight Test

The antenna system was programmed to run with the same sequence of driving signals as the previous day. The reference sensor station was re-configured to use the same sensors but with a different data acquisition system, as the primary DACQ was now in the helicopter (see the attached drawings). The platform and primary data acquisition system was attached to the aircraft, and tested to verify proper operation (Figure 3). A long term data acquisition session was then launched, and the aircraft readied for takeoff.

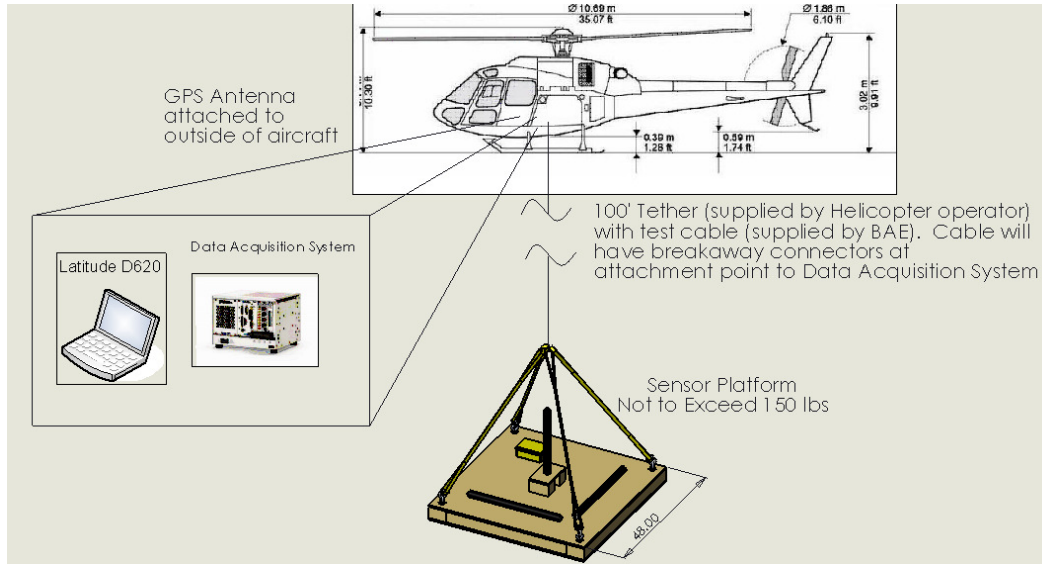


Figure 8

The helicopter lifted off and flew to the point over the middle of the antenna. The aircraft established itself at an altitude of approximately 400 ft and hovered. We waited for the sensor platform to stabilize, recorded the time, and waited 10 min. This was repeated for aircraft altitudes of 1000', 2000' and 3000'. Note that with the 100' tether, this gives sensor altitudes of 300' [91 m], 900' [274 m], 1900' [579 m] and 2900' [884 m]. Unfortunately, during the flight, the connection from the sensor package to the DACQ came loose during the flight. Note that for safety reasons, the sensor platform must be rigged such that it will break away cleanly from the aircraft if the emergency release is used. For this reason, the umbilical connection was a friction fit connector, and this was where the connection was lost.

Checking the data showed that this happened approximately 15 minutes into the flight, just before valid antenna data was acquired. However, the positive result from evaluating this data showed that the flight generated noise was small enough that it did not cause saturation of the sensors, and did not significantly interfere with the frequencies of interest as it was dominated by low frequencies. The test was then repeated, with essentially the same procedure but with shortened time scales. The data acquisition time at each altitude was shortened to 5 minutes, and Table 2 shows the modified antenna operating parameters.

Duration (sec)	Mode	Frequency	Voltage (Vrms)	Current (Irms)
5	Off	-	-	-
40	Square	217 Hz	69	9.6
5	Off			
40	Square	217 Hz	69	9.6
5	Off			
40	Square	217 Hz	69	9.6
5	Off			
40	Square	217 Hz	69	9.6

5	Off			
20	Sine	1000 Hz	48	6.2
20	Sine	3000 Hz	47	4.1
20	Sine	10000 Hz	47	1.6

Table 2